

# On the Metric of Charge Transfer Molecular Excitations: A Simple Chemical Descriptor

Ciro A. Guido,<sup>\*,†</sup> Pietro Cortona,<sup>†</sup> Benedetta Mennucci,<sup>‡</sup> and Carlo Adamo<sup>\*,§,||</sup>

<sup>†</sup>Laboratoire Structures, Propriétés et Modélisation des Solides (SPMS), CNRS UMR 8580, École Centrale Paris, Grande Voie des Vignes, F-92295 Châtenay-Malabry, France

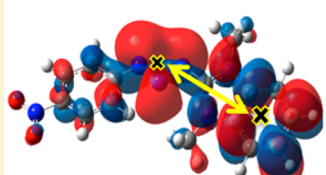
<sup>‡</sup>Department of Chemistry, University of Pisa, Via Risorgimento 35, 56126 Pisa, Italy

<sup>§</sup>Laboratoire d'Électrochimie, Chimie des Interfaces et Modélisation pour l'Énergie, CNRS UMR-7575, Chimie ParisTech, 11 rue P. et M. Curie, F-75231 Paris Cedex 05, France

<sup>||</sup>Institut Universitaire de France, 103 Bd Saint-Michel, F-75005 Paris, France

## S Supporting Information

**ABSTRACT:** A new index is defined with the aim of further exploring the metric of excited electronic states in the framework of the time-dependent density functional theory. This descriptor, called  $\Delta r$ , is based on the charge centroids of the orbitals involved in the excitations and can be interpreted in term of the hole–electron distance. The tests carried out on a set of molecules characterized by a significant number of charge-transfer excitations well illustrate its ability in discriminating between short ( $\Delta r \leq 1.5$  Å) and long-range ( $\Delta r \geq 2.0$  Å) excitations. On the basis of the well-known pitfalls of TD-DFT, its values can be then associated to the functional performances in reproducing different type of transitions and allow for the definition of a “trust radius” for GGA and hybrid functionals. The study of other systems, including some well-known difficult cases for other metric descriptors, gives further evidence of the high discrimination power of the proposed index. The combined use with other density or orbital-based descriptors is finally suggested to have a reliable diagnostic test of TD-DFT transitions.

$$R_{ia} = \left| \langle \phi_a(\mathbf{r}) | \mathbf{r} | \phi_a(\mathbf{r}) \rangle - \langle \phi_i(\mathbf{r}) | \mathbf{r} | \phi_i(\mathbf{r}) \rangle \right|$$
$$\Delta r = \frac{\sum_{i,a} K_{ia}^2 R_{ia}}{\sum_{i,a} K_{ia}^2}$$

$$\Delta r < 1.5 \text{ Å}$$

↓  
short range

## 1. INTRODUCTION

The study of electronic excited states is one of the major issues in physics, chemistry, biology, and material science due to their relevance to both fundamental science and technological applications.<sup>1,2</sup> Many factors, such as technical setups, short lifetimes, and entangled properties, could make their experimental characterization difficult and sometimes not fully irrefutable. This situation is even more involved since, in the absence of a precise physical definition, the description of the electronic transitions in terms of their nature (valence, charge transfer, etc.) is made on an empirical basis. It is not surprising, therefore, that a great benefit has been derived from theoretical analysis, since the dawn of modern quantum chemistry.<sup>3</sup>

One of the major issues in calculating excited-state energies and related properties is the computational cost affecting the chosen computational method. From one side, it is well-known that post-Hartree–Fock (HF) methods, accurately describing the electronic correlation, are too expensive for medium and large size molecules,<sup>4</sup> despite the enormous progress made during the last years to improve their speeding-up (see, for instance, ref 5). On the other hand, time dependent density functional theory (TD-DFT), proposed more than 25 years ago,<sup>6</sup> emerged as a promising approach to the study of excited states, and experience has shown that TD-DFT excitation energies are generally in (very) good agreement with experiments (see, for instance, ref 7). As a matter of fact, the

optimal compromise between accuracy and computational cost makes TD-DFT the most widely used method of calculating excitation energies of chemically relevant molecules.

However, the linear response (LR) formulation of TD-DFT<sup>8</sup> sums up the typical problems of ground state DFT<sup>9</sup> with those originating in the LR approximation and the adiabatic assumption.<sup>10,11</sup> These approximations do not significantly affect the calculation of electronic transitions involving valence electrons (valence excitations) which, as extensively shown in literature (see, for instance, refs 12–16), are accurately reproduced. On the contrary, numerous numerical benchmarks showed that the LR-TD-DFT approach, combined with approximate exchange–correlations functionals (XCFs), meets some difficulties in describing charge transfer (CT) excitations, multielectron excitations, and absorption spectra of systems with delocalized or not-paired electrons.<sup>16–19</sup>

These results not only indicate that TD-DFT is far from being a “black-box” approach as sometimes is believed but also point out the need of a diagnostic tool giving a numerical indication of the nature of the computed transition (e.g., valence vs CT) and warning the user when the selected method is no longer applicable or prone to significant errors. This latter feature is even more important in view of the large number of

Received: April 25, 2013

Published: May 29, 2013

computational applications involving TD-DFT, sometimes carried out by nonspecialists.

The development of what can be defined as a metric of excited states is not straightforward, but several examples can be found in literature.<sup>20–25</sup> They include geometrical descriptors as well as indexes based on the analysis of the molecular orbitals or the electron densities. All these descriptors have pros and cons, but only few of them have been used as diagnostic tools in order to monitor TD-DFT results.<sup>20,22</sup> Among others and of particular interest for this paper, the  $\Lambda$ -index should be mentioned, based on the overlap of molecular orbital moduli.<sup>20</sup> This index has been successfully used as a diagnostic tool,<sup>26,27</sup> but as it was pointed out by its authors, it is not able to individuate problematic excitations in some difficult cases.<sup>28</sup>

In this context, a new index, called  $\Delta r$ , has been developed in order to provide a new tool for exploring the excited-state metric. This index, based on the charge centroids of the orbitals involved in the transition, can be easily interpreted, since it measures the average hole–electron distance upon excitation. The aim is to use this index as a diagnostic tool giving some indications about the expected accuracy of the excitation energies computed by TD-DFT and on the nature of the electronic transitions under investigation.

In order to assess the ability of this descriptor in accomplishing these tasks, a molecular training set, characterized by valence and CT excitations, has been considered together with 12 functionals belonging to different rungs of the Perdew ladder.<sup>29</sup> Its indications have been compared to those provided by the  $\Lambda$ -index. The subsequent study of some difficult cases will then show that  $\Delta r$  still provides valuable information when the  $\Lambda$  index seems to fail.

## 2. THEORY

In the Kohn–Sham approach to the linear response of TD-DFT formulation,<sup>8</sup> a non-Hermitian eigenvalue problem has to be solved:

$$\begin{bmatrix} A & B \\ B & A \end{bmatrix} \begin{bmatrix} X \\ Y \end{bmatrix} = \omega \begin{bmatrix} 1 & 0 \\ 0 & -1 \end{bmatrix} \begin{bmatrix} X \\ Y \end{bmatrix} \quad (1)$$

where the Lagrange multiplier  $\omega$  contains the excitation energies for the transitions from the ground to excited states. The matrix elements of the electronic Hessian in the case of a hybrid functional ( $C_{\text{HF}}$  is the coefficient of the HF-exchange, HFX) take the form

$$A_{ia\sigma,jb\tau} = \delta_{ij}\delta_{ab}\delta_{\sigma\tau}(\epsilon_a - \epsilon_i)^2 + \langle i_{\sigma}j_{\tau} | a_{\sigma}b_{\tau} \rangle - C_{\text{HF}}\delta_{\sigma\tau}\langle i_{\sigma}a_{\sigma} | j_{\tau}b_{\tau} \rangle + (1 - C_{\text{HF}})\langle i_{\sigma}j_{\tau} | f_{\text{xc}} | a_{\sigma}b_{\tau} \rangle \quad (2)$$

$$B_{ia\sigma,jb\tau} = \langle i_{\sigma}b_{\tau} | a_{\sigma}j_{\tau} \rangle - C_{\text{HF}}\delta_{\sigma\tau}\langle i_{\sigma}a_{\sigma} | b_{\tau}j_{\tau} \rangle + (1 - C_{\text{HF}})\langle i_{\sigma}b_{\tau} | f_{\text{xc}} | a_{\sigma}j_{\tau} \rangle \quad (3)$$

where

$$\langle p_{\sigma}q_{\sigma} | r_{\tau}s_{\tau} \rangle = \iint \frac{\varphi_p^*(r)\varphi_q^*(r')\varphi_r(r)\varphi_s(r')}{|r - r'|} dr dr' \quad (4)$$

$$\langle p_{\sigma}q_{\sigma} | f_{\text{xc}} | r_{\tau}s_{\tau} \rangle = \iint \varphi_p^*(r)\varphi_q^*(r')f_{\text{xc}}(r, r')\varphi_r(r)\varphi_s(r') dr dr' \quad (5)$$

The molecular orbitals ( $\varphi$ ) indexes follow the usual convention:  $i, j, k, l, \dots$  for occupied;  $a, b, c, d, \dots$  for virtual;  $p, q, r, s, \dots$  for generic orbitals;  $\sigma, \tau$  for spin. In the case of intermolecular CT, for which the product function  $\varphi_i(\mathbf{r})\varphi_a(\mathbf{r}) \rightarrow 0$ , Dreuw et al.<sup>11</sup> showed that

$$A_{ia\sigma,jb\tau} = \delta_{ij}\delta_{ab}\delta_{\sigma\tau}(\epsilon_a - \epsilon_i)^2 - C_{\text{HF}}\delta_{\sigma\tau}\langle i_{\sigma}a_{\sigma} | j_{\tau}b_{\tau} \rangle \quad (6)$$

$$B_{ia\sigma,jb\tau} = 0 \quad (7)$$

Starting from this consideration, a diagnostic index, based on the molecular orbital moduli involved in the electronic transition, was proposed:<sup>20</sup>

$$\Lambda = \frac{\sum_{ia} K_{ia}^2 \int |\varphi_a(\mathbf{r})||\varphi_i(\mathbf{r})| d\mathbf{r}}{\sum_{ia} K_{ia}^2} \quad (8)$$

where

$$K_{ia} = X_{ia} + Y_{ia} \quad (9)$$

includes both excitation ( $X_{ia}$ ) and de-excitation ( $Y_{ia}$ ) coefficients. This index has been used as a diagnostic tool, and it has been suggested that below determined thresholds (0.3 for hybrid and 0.4 for GGA functionals) the orbital overlap is small and the obtained excitations should be discharged.<sup>20</sup>

Its applications include analysis of CT transitions,<sup>26,27,30</sup> oscillator strengths,<sup>31</sup> potential energy surfaces,<sup>32</sup> and more recently, triplet instabilities.<sup>33</sup> However, as pointed out by the authors themselves,<sup>28,34</sup> even if the index correctly identified several low-overlap and problematic excitations, it is unable to identify other failures associated to spatially extended orbitals, such as in the case of triazenes.<sup>28</sup> The same holds for others systems, including *N*-phenylpyrrole already present in the original test set.<sup>20,35,36</sup> As it has been pointed out, “ $\Lambda$  does not sound the alarm when a charge-transfer like situation arises, because the spatial overlap between the original orbitals is not small”.<sup>37</sup>

This behavior can be correlated to the dependency of bielectronic terms in the matrices **A** and **B** (eqs 2 and 3) on the product  $\varphi_i(\mathbf{r})\varphi_a(\mathbf{r})$  at each point  $\mathbf{r}$  of the integration domain. If the electronic transition involves orbitals in different regions of space, a very small value of  $\Lambda$  implies  $\varphi_i(\mathbf{r})\varphi_a(\mathbf{r}) \rightarrow 0$  and then a small value of the bielectronic integrals of type  $\langle ij | lab \rangle$  and  $\langle j | f_{\text{xc}} | lab \rangle$ . For the other cases, on the contrary, there is not a simple relation between  $\Lambda$  and the bielectronic terms. Therefore the absolute overlap diagnostic can work properly only for low values ( $\Lambda \leq 0.3$ ), i.e., in high charge transfer regime, in other words, with a long-range character. On the other hand, excitations that are short ranged in character involve close occupied-virtual orbital pairs, and therefore very large values of  $\Lambda$  could be associated.

From another point of view Ziegler and co-workers<sup>21</sup> suggested that the GGA Hessian can be used to describe changes in energy due to small perturbations of electron density, but it is not suitable for one-electron excitations involving density rearrangement of a full electron charge. In contrast, the HF Hessian describes larger perturbations to electron density, also due to the complete self-interaction cancellation by means of exact exchange, and, of course, an intermediate behavior is expected for hybrid functionals.<sup>21</sup>

Therefore, an index able to describe the amount of this spatial rearrangement could warn the user when the XCF is inadequate: intuitively, one expects a small variation of electron

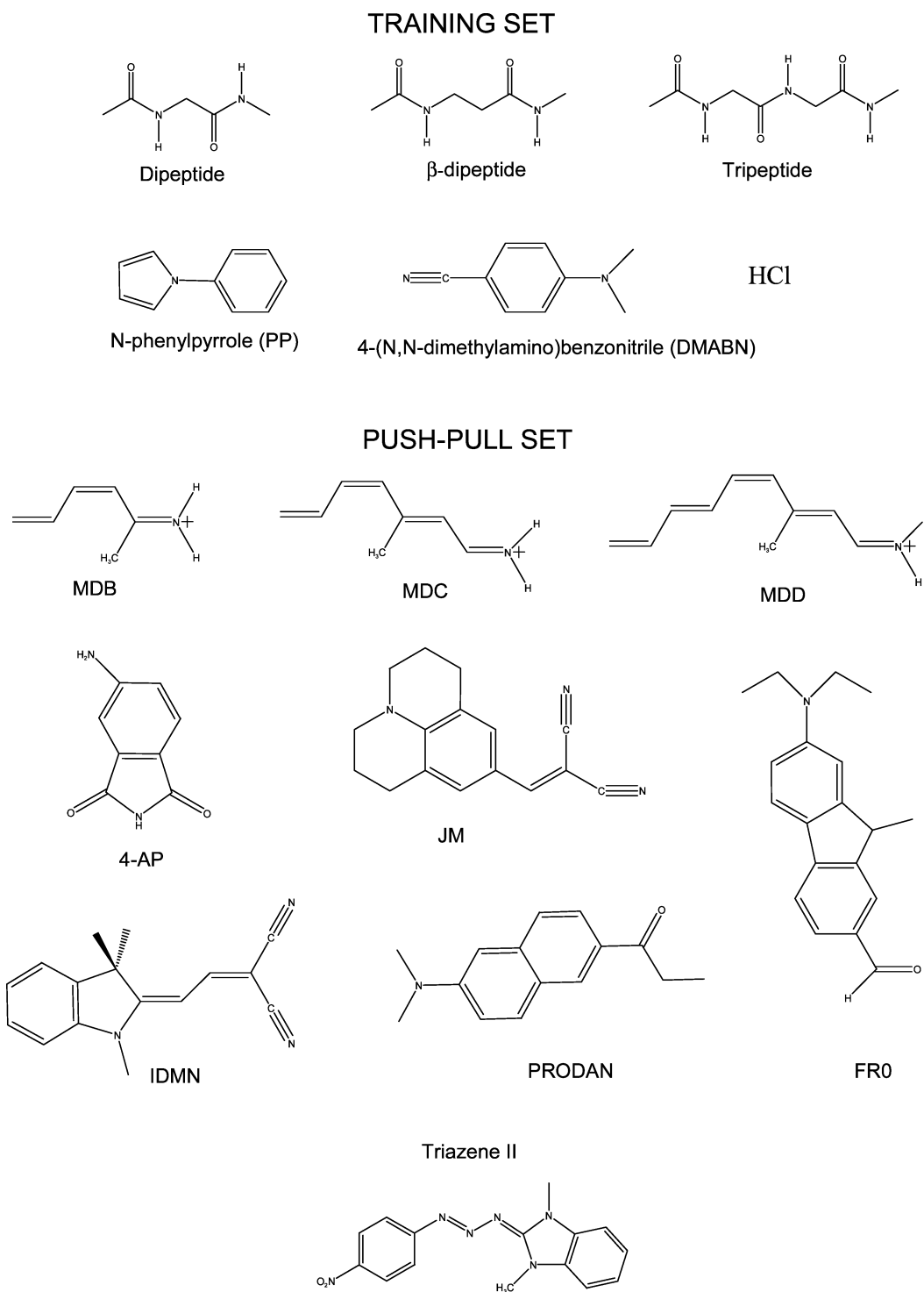


**Figure 1.** Molecular sets considered in the present study.

density for local valence excited states and higher values in the case of CT states.

The hole–particle pair interactions could be related to the distance covered during the excitations, so one possible descriptor could be their average distance, weighted in function of the excitation coefficients. The following definition will be then introduced:

$$\Delta \mathbf{r} = \frac{\sum_{ia} K_{ia}^2 |\langle \varphi_a | \mathbf{r} | \varphi_a \rangle - \langle \varphi_i | \mathbf{r} | \varphi_i \rangle|}{\sum_{ia} K_{ia}^2} \quad (10)$$

where  $|\langle \varphi_i | \mathbf{r} | \varphi_i \rangle|$  is the norm of the orbital centroid.<sup>38</sup> It should be remarked that the basic components of the index, orbital centroids, are broadly used in quantum chemistry. Indeed they found many applications in the field of localized orbitals, as for instance in the well-known Boys' localization or, more recently, for the modeling of dispersion forces.<sup>39–41</sup> Furthermore, orbital centroids are traditionally computed in many quantum chemical codes or, eventually, their implementation is straightforward. For sake of simplicity this descriptor will be simply indicated as  $\Delta \mathbf{r}$ -index and it will be expressed in Å.

### 3. BENCHMARK SETS AND COMPUTATIONAL DETAILS

All DFT and TD-DFT calculations have been carried out with a locally modified version of the GAUSSIAN development program,<sup>42</sup> where the diagnostic indexes  $\Lambda$  and  $\Delta r$  were implemented.

Three test sets (see Figure 1), including molecules having different types of excitations, have been chosen. The first (training) set includes all the systems used by Peach et al.<sup>20</sup> to define the  $\Lambda$  index and presenting challenging CT excitations, namely: a model dipeptide, longer chains  $\beta$ -dipeptide and tripeptide, *N*-phenylpyrrole (PP), 4-(*N,N*-dimethylamino)-benzonitrile (DMABN), and HCl. The second set, issued from our precedent benchmark sets for excited state geometry optimizations,<sup>43,44</sup> contains some push–pull chromophores, i.e., extended systems with charge delocalization: 4-aminophthalimide (4-AP), julolidine-malononitrile (JM), indolinedimethine-malononitrile (IDMN), 6-propionyl-2-dimethylamino naphthalene (PRODAN), 7-dimethylamino-9,9-dimethyl-9-H-fluorene-2-carbaldehyde (FR0), and three model systems of a protonated Schiff's base (MDB, MDC, and MDD), used as prototype models of retinal chromophore. Finally, Triazene II, a particularly difficult case for TD-DFT and excited state descriptors,<sup>20,45</sup> has been considered.

The basis sets used in previous works were chosen. In particular, for the training set, the cc-pVTZ basis set and 12 different XC functionals were considered. These functionals span over different rungs of the Perdew Ladder<sup>29</sup> and include two generalized-gradient approximations (GGA), PBE<sup>46</sup> and BLYP;<sup>47,48</sup> one meta-GGA, TPSS;<sup>49</sup> five global hybrids (GH), PBE0,<sup>50</sup> B3LYP,<sup>51</sup> BH&HLYP,<sup>52</sup> TPSSH,<sup>53</sup> and PBE0-1/3;<sup>54</sup> four and Range-Separated Hybrid (RSH) functionals, LC- $\omega$ PBE,<sup>55</sup> LC-TPSS,<sup>56</sup> CAM-B3LYP,<sup>57</sup> and LC- $\omega$ PBEh.<sup>58</sup> The PBE0, B3LYP, and CAM-B3LYP functionals were used for the push–pull set with the 6-311++G(d,p) basis set, while the 6-311+G(2d,p) basis and PBE, PBE0, and CAM-B3LYP were considered for Triazene II.

The TD-DFT errors were defined with respect to reference values taken from literature. In particular, results of Complete Active Space second-order Perturbative Theory (CASPT2) were considered for model peptides, while CC2/cc-pVTZ calculations are the references for PP and DMABN.<sup>20</sup> RI-CC2/aug-cc-pVTZ and RI-CC2/def-QZVPP results were considered for the push–pull set and Triazene II, respectively.<sup>20,44</sup>

The structures reported in the benchmark repository were used when possible.<sup>59</sup> In the other cases, the geometries were optimized using the same functional (and basis set) as in the calculation of the electronic transitions.

### 4. RESULTS AND DISCUSSION

As a first step, a benchmark study of transition energies and  $\Lambda$ -index was carried out on a training set, composed by the vertical electronic transitions associated to the molecule sketched in Figure 1. Albeit the results reported in Table 1 are far from being exhaustive in a statistical sense, they are in global agreement with those provided by more extensive studies.<sup>12,13</sup> Indeed, GHs provide the lowest errors in valence excitations, while they underestimate CT vertical excitation energies. The introduction of a range-separated scheme partially corrects this behavior, and the lowest deviations are obtained with LC- $\omega$ PBEh and CAM-B3LYP. Indeed, the

**Table 1.** Mean Absolute Error (MAE), Standard Deviation (SD), Maximum Positive (Max+) and Negative (Max–) Errors for the Valence (V) and Charge Transfer (CT) Excitations for the Training and Push–Pull Sets (see Figure 1 for definition of the sets)<sup>a</sup>

| Training Set (24 excitations) <sup>b</sup> |               |                |               |             |       |       |
|--|---------------|----------------|---------------|-------------|-------|-------|
| functional                                 | MAE-V<br>(10) | MAE-CT<br>(14) | MAE-<br>Total | SD<br>Total | Max+  | Max-  |
| PBE  | 0.26          | 2.60           | 1.62          | 1.58        | 0.31  | −5.04 |
| PBE0                                       | 0.16          | 1.06           | 0.69          | 0.76        | 0.53  | −2.79 |
| PBE0-1/3                                   | 0.26          | 0.66           | 0.50          | 0.45        | 0.63  | −2.14 |
| LC- <i>ω</i> PBE                           | 0.29          | 0.71           | 0.53          | 0.42        | 1.47  | −0.87 |
| LC- <i>ω</i> PBEh                          | 0.31          | 0.17           | 0.22          | 0.17        | 0.76  | −0.40 |
| BLYP                                       | 0.27          | 2.61           | 1.64          | 1.57        | 0.30  | −5.03 |
| B3LYP                                      | 0.16          | 1.34           | 0.85          | 0.88        | 0.46  | −3.18 |
| BH&HLYP                                    | 0.43          | 0.32           | 0.37          | 0.23        | 0.89  | −0.40 |
| CAM-B3LYP                                  | 0.22          | 0.27           | 0.25          | 0.21        | 0.66  | −0.75 |
| TPSS                                       | 0.21          | 2.39           | 1.48          | 1.50        | 0.49  | −4.78 |
| TPSSh                                      | 0.26          | 1.88           | 1.20          | 1.19        | 0.61  | −3.93 |
| LC-TPSS                                    | 0.43          | 1.19           | 0.87          | 0.62        | 1.95  | none  |
| Push–Pull Set (7 excitations) <sup>c</sup> |               |                |               |             |       |       |
| functional                                 | MAE-Total     |                | SD            | Max+        | Max−  |       |
| PBE0                                       | 0.15          |                | 0.07          | 0.22        | −0.21 |       |
| B3LYP                                      | 0.18          |                | 0.16          | 0.48        | −0.16 |       |
| CAM-B3LYP                                  | 0.26          |                | 0.10          | none        | −0.40 |       |

<sup>a</sup>All values are in eV. <sup>b</sup>CASPT2, CC2 and gas phase reference values issued from ref 16. <sup>c</sup>RI-CC2 reference values issued from ref 36.

combination of GH and range separation seems to be particularly effective in such cases.<sup>60–62</sup>

More in detail, the PBE and BLYP performances are very similar, with relatively good results for valence excitations but very high errors for CT. The introduction of the kinetic energy dependence in the meta-GGA TPSS functional reduces to 0.2 eV the MAE for CT excitations, which remains nevertheless above 2 eV. Moreover, for most of the excitations, except those of HCl and DMABN ones, the CT absolute errors of PBE, BLYP, TPSS, and TPSSH are greater than 1 eV. In going from GGAs to GHs with 20–25% of HFX (B3LYP, PBE0), the MAEs for valence and CT excitations are reduced to about 50%. However, in the CT case, a half of the excitations have absolute errors greater than 1 eV (see Supporting Information for details). As expected, the increase of the HFX percentage induces a better description of CT excitations: the MAE decreases from 1.06 to 0.66 eV in going from PBE0 to PBE0-1/3 and from 1.34 to 0.32 eV from B3LYP to BH&HLYP. Finally, in the case of the push–pull set, better performances are obtained using GHs (PBE0 and B3LYP) instead of RSH (CAM-B3LYP), even if the difference in MAE is less than 0.1 eV and SD values show that performances are not really different (see Table 1).

In view of the unbalanced weight of the relative number of valence and charge transfer excitations and of the expected accuracies for the two sets (around 0.2 eV for the first and around 0.7 for the second) an absolute value of 0.5 eV will be considered as an average threshold of accuracy. In other terms, a transition showing an error above this threshold will be considered as not correctly reproduced in the following discussion.

The results for the  $\Lambda$ -index are plotted in Figure 2, where the errors ( $\Delta E$ ) are reported as a function of  $\Lambda$  for the training data set. As a first remark it should be noted that, independently of

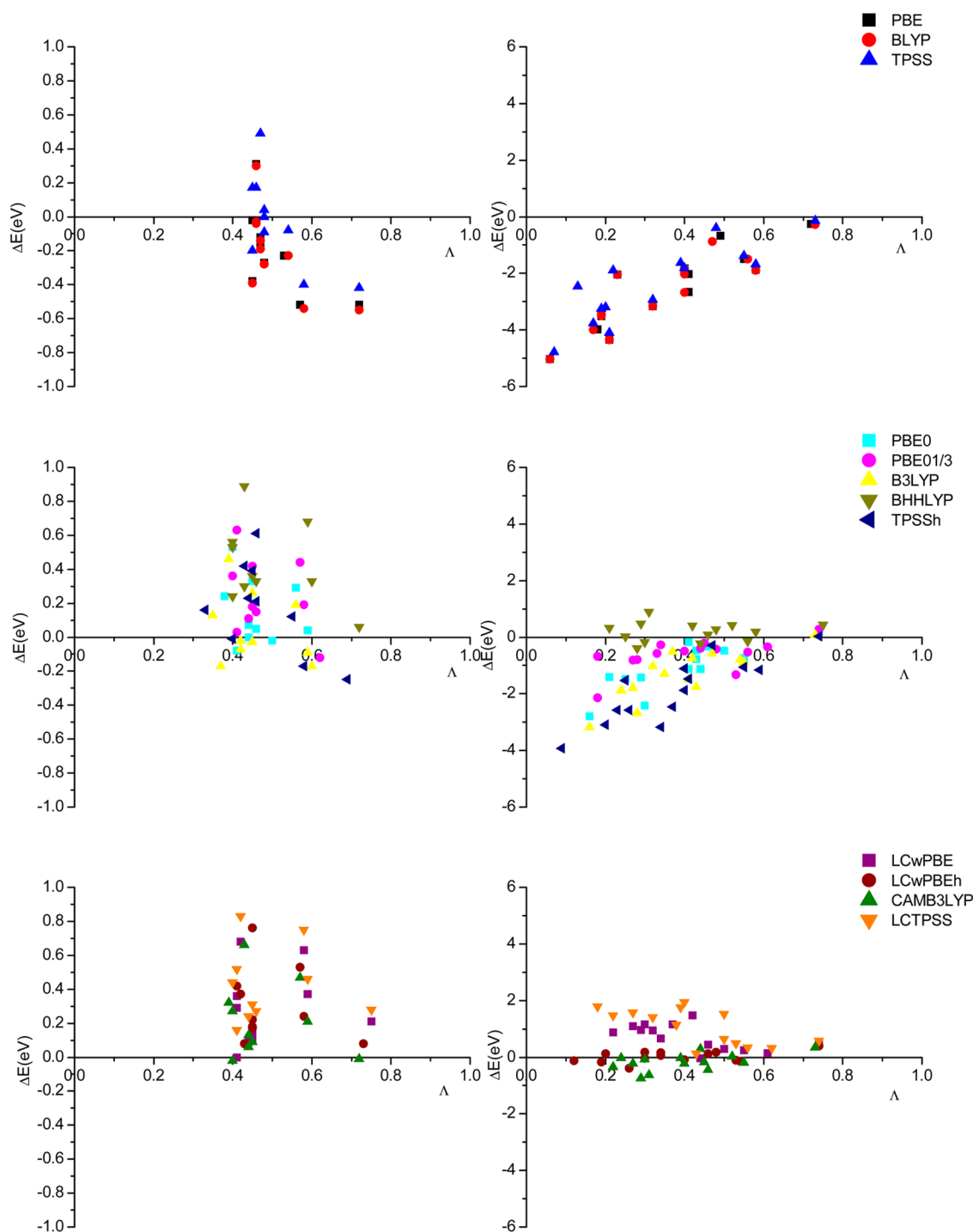


**Figure 2.** Excitation energy errors ( $\Delta E$ , eV) plotted against the  $\Lambda$ -index for the training set. Left side: valence excitations; right side: charge transfer excitations. Top: GGA and meta-GGA functionals; middle: global and meta-GGA hybrids; bottom: range separate hybrids.

the functional,  $\Lambda$  is always in the range  $0.3 \leq \Lambda \leq 0.8$  for valence excitations (left part of the figure). Furthermore, most of the excitations fall in a smaller interval, ranging from 0.4 to 0.6. As previously pointed out by Peach et al.,<sup>20</sup> the calculated transition energies are quite accurate. GGA approximations give absolute errors generally smaller than 0.5 eV. Increasing the HF exchange percentage, the  $\Delta E$ s are shifted toward larger values, and some excitation energies have errors greater than the chosen threshold (0.5 eV). A clear discrepancy between the indications provided by  $\Lambda$  and the large errors thus appears. Concerning the CT excitations (Figure 2, right), the  $\Lambda$  values

cover a larger interval ( $0.1 \leq \Lambda \leq 0.8$ ). In this range the errors are almost independent from the value of  $\Lambda$  for range-separated functionals and global hybrids with a high HFX percentage (BH&HLYP and PBE0-1/3), while there is a clear increase of the errors with the decreasing of  $\Lambda$  for GGAs, TPSS, and GHs with a HFX contribution smaller than 33%. Indeed, as already noted in ref 20, several excitations in the range  $0.4 \leq \Lambda \leq 0.6$  with  $|\Delta E| > 0.5$  are found. The  $\Lambda$  index cannot distinguish, therefore, CT from valence excitations in these systems.

With these results as reference, the second step of the study was to assess the new index,  $\Delta r$ . In Figure 3, the errors in



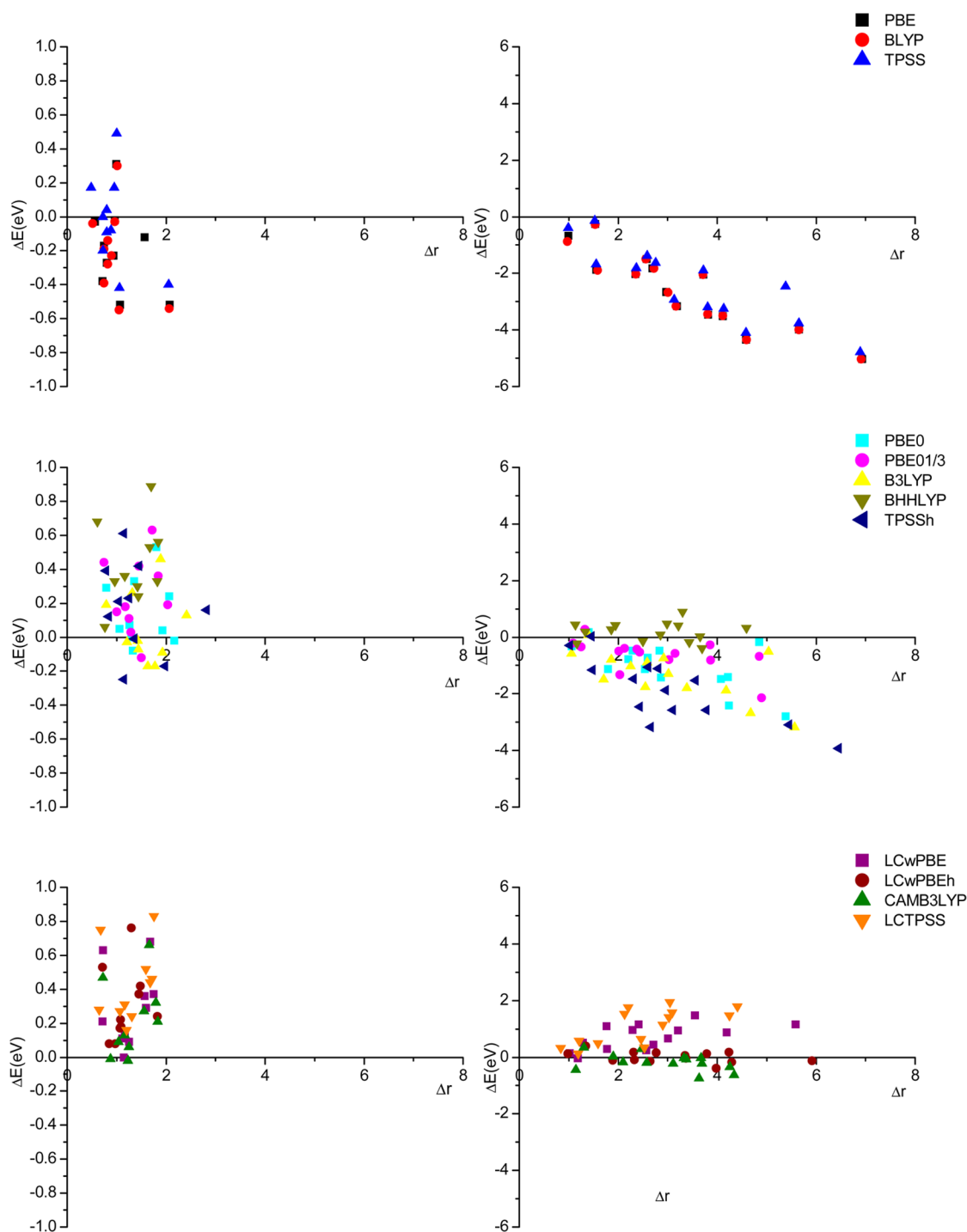


**Figure 3.** Excitation energy errors ( $\Delta E$ , eV) plotted against the  $\Delta r$ -index ( $\text{\AA}$ ) for the training set. Left side: valence excitations; right side: charge transfer excitations. Top: GGA and meta-GGA functionals; middle: global and meta-GGA hybrids; bottom: range separate hybrids.

excitation energies are plotted as a function of  $\Delta r$ . First, the different behaviors of the various functionals for the valence excitations subset should be noted (left side of the figure). GGA functionals give  $0.5 \text{ \AA} \leq \Delta r \leq 2.0 \text{ \AA}$ , with most values between 0.5 and 1  $\text{\AA}$ . The  $\Delta r$  range is slightly larger for GHs,  $0.5 \text{ \AA} \leq \Delta r \leq 3.0 \text{ \AA}$ , but most of the values are smaller than 2  $\text{\AA}$ . Finally, RSHs are strictly confined in the interval  $0.5 \text{ \AA} \leq \Delta r \leq 2.0 \text{ \AA}$ .

Analyzing the CT excitations (right side of Figure 3), it appears that, for GGA, meta-GGA, and GHs with HFX percentage lower than 33%, errors increase with the increasing

of the distance covered during the excitation:  $|\Delta E| > 0.5 \text{ eV}$  if  $\Delta r > 1 \text{ \AA}$  for GGA and meta-GGA, or if  $\Delta r > 1.5 \text{ \AA}$  for GHs. This threshold value increases for larger HF contributions, and it becomes 2  $\text{\AA}$  in the case of PBE0-1/3. As expected, 50% of HFX allows for obtaining good CT excitation energies, with errors in the range of  $\pm 0.5 \text{ eV}$  almost independent of the distance, as for RSH functionals. These findings seem physically sound: failures in describing excitations involving hole–electrons separations greater than 1.5  $\text{\AA}$  could be expected for GGAs, meta-GGAs, and GHs functionals with low HFX percentage. In these cases, RSHs or GHs with a high HFX

exchange percentage should be used. It should be noticed that a similar threshold (1.6 Å) has been suggested on the basis of the analysis of electron density variations.<sup>22</sup> Moreover, since TD-DFT excitations are sensible to basis set effects,<sup>63</sup> a (slight) extension of the upper bound of  $\Delta r$  upon inclusion of diffuse functions is expected. Therefore the interval 1.5–2.0 Å will be retained as a threshold.

A direct comparison of the two indexes,  $\Lambda$  and  $\Delta r$ , is reported in Figure 4, where  $1/\Delta r$  (in Å<sup>-1</sup>) is plotted as a

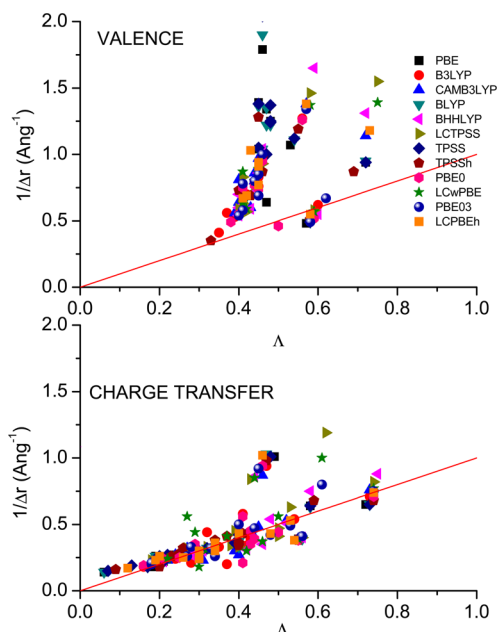


**Figure 4.** Correlation plot of  $1/\Delta r$  (Å<sup>-1</sup>) against the  $\Lambda$ -index, over the training set. Red lines represent a perfect (1:1) linear correlation.

function of  $\Lambda$ . First it should also be noted that most of the  $\Lambda$ -index values for the valence and CT excitations are in the range 0.4–0.6, which clearly shows its low discrimination power. The  $\Delta r$  index provides a clearer indication of the excitation type (valence or CT), differentiating these middle range  $\Lambda$ -values in short- and long-range (top and bottom panels of Figure 4). Only CT transitions, i.e., when  $0.1 \leq \Lambda \leq 0.6$  and  $1/\langle \Delta r \rangle < 0.66$  Å<sup>-1</sup> ( $\Delta r > 1.5$  Å), is a linear correlation found (Figure 4, bottom).

In order to further test the proposed  $\Delta r$ -index, some push–pull systems have been considered (see Figure 1 for the structures). The results obtained with selected functionals (a GH, PBE0, and a RSH, CAM-B3LYP) are plotted in Figure 5. These functionals provide quite accurate values of the vertical excitation energies, with deviations smaller than 0.5 eV with respect to the RI-CC2 results. This is not surprising, since all the indexes are within the recommended limits: all the  $\Lambda$ -values are greater than 0.4 and all the  $\Delta r$ -values (with two only exceptions) are below 2.0 Å.

An even more stringent test is represented by Triazene II, whose seven lowest transitions are collected in Table 2. The results reported in the table and the upper part of Figure 6 clearly show that the  $\Lambda$ -index does not provide a clear indication of the functional performances, as it was previously pointed out in ref 31. Indeed, the  $\Lambda$  values are in many cases above the threshold of 0.3/0.4, and one should expect a good behavior with both GGA and GH functionals but instead errors as large as 2.0 eV are found for PBE (0.8 eV for PBE0). In

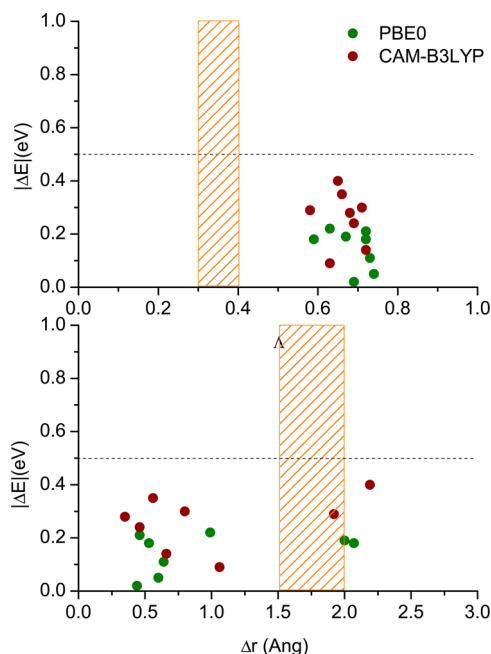


**Figure 5.** Absolute deviations ( $|\Delta E|$  in eV) of excitation energies for the push–pull set as function of the  $\Lambda$  and  $\Delta r$  indexes. Dashed areas represented the recommended thresholds for the two indexes.

contrast, the  $\Delta r$ -index indicates that all these excitations involve a hole–electron distance greater than 2.0 Å, and large errors can be expected for non-RSH functionals: in these cases CAM-B3LYP should be used in order to obtain accurate results, and this is indeed confirmed. In other words, for Triazene II the  $\Delta r$ -index is successful while the  $\Lambda$ -index fails.

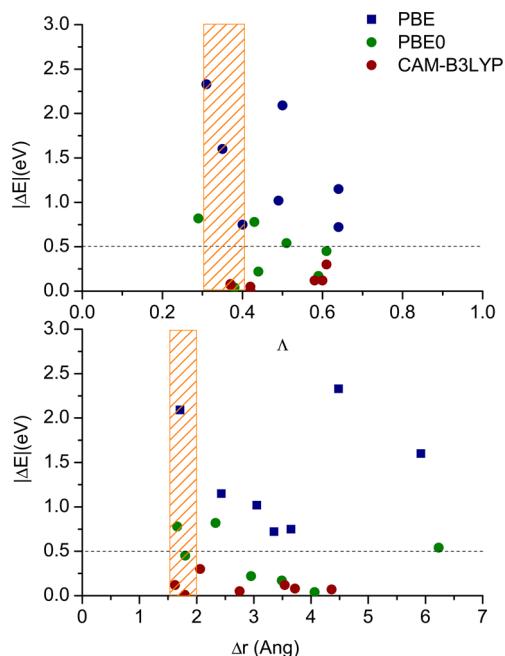
## 5. FINAL COMMENTS AND CONCLUSIONS

The definition of a molecular excitation metric and its relationship to TD-DFT performances is of particular relevance since descriptors, as the one proposed in the present paper, can give at first glance a (semi)quantitative evaluation of the expected result accuracy. The proposed index,  $\Delta r$ , is particularly attractive since it is based on some simple and chemically intuitive quantities such as orbital centroids. Indeed, its interpretation in chemical terms is simple since it measures the average hole–electron separation upon the electronic excitation. This distance is related to the nature of the transition, since valence excitations are characterized by short distances, while usually larger distances are found for CT excitations. In turn large distances very often imply large TD-DFT errors, depending on the nature of the exchange–correlation functional used. Indeed a “trust radius” for  $\Delta r$ , in the sense of Ziegler and co-workers,<sup>21</sup> can be defined so that sufficiently accurate results are expected for excitations characterized by  $\Delta r$  values below the 2.0 Å threshold (1.5 Å for GGA functionals). In contrast, larger  $\Delta r$  indicate that a high error in the associate transition energies is alike. In such a case ( $\Delta r > 2.0$  Å), the use of RSH or GH with a high ( $\geq 33\%$ ) HF exchange percentage is mandatory, as already suggested in the literature.<sup>12,13</sup>

The interest of the  $\Delta r$ -index resides in its chemical and simple metric which is associated to a simple pictorial concept (hole–electron separation) and in the straightforward evaluation at negligible computational cost. A clear definition of a convergence limit makes its use simple and, as above showed,

Table 2. TD-DFT Vertical Excitation Energy Differences ( $\Delta E$ , in eV) with Respect to RI-CC2 Values and Diagnostic Indexes for Triazene II

| exc. | ref <sup>a</sup> | PBE        |           |            | PBE0       |           |            | CAM-B3LYP  |           |            |
|------|------------------|------------|-----------|------------|------------|-----------|------------|------------|-----------|------------|
|      |                  | $\Delta E$ | $\Lambda$ | $\Delta r$ | $\Delta E$ | $\Lambda$ | $\Delta r$ | $\Delta E$ | $\Lambda$ | $\Delta r$ |
| i    | 3.03             | -1.02      | 0.49      | 3.05       | -0.22      | 0.44      | 2.95       | 0.05       | 0.42      | 2.75       |
| ii   | 3.34             | -0.72      | 0.64      | 3.35       | -0.17      | 0.59      | 3.49       | 0.12       | 0.58      | 3.54       |
| iii  | 3.90             | -0.75      | 0.40      | 3.65       | -0.04      | 0.38      | 4.06       | 0.07       | 0.37      | 4.36       |
| iv   | 4.53             | -1.15      | 0.64      | 2.43       | -0.45      | 0.61      | 1.80       | 0.12       | 0.60      | 1.62       |
| v    | 5.00             | -2.09      | 0.50      | 1.71       | -0.78      | 0.43      | 1.66       | 0.30       | 0.61      | 2.06       |
| vi   | 5.04             | -1.60      | 0.35      | 5.92       | -0.54      | 0.51      | 6.23       | 0.01       | 0.42      | 1.79       |
| vii  | 6.02             | -2.33      | 0.31      | 4.48       | -0.82      | 0.29      | 2.33       | -0.08      | 0.37      | 3.72       |

<sup>a</sup>From ref 20.Figure 6. Absolute deviations ( $\Delta E$  in eV) of Triazene II excitation energies as a function of the  $\Lambda$  and  $\Delta r$  indexes. Dashed areas represented the recommended thresholds for the two indexes.

reliable. When possible, it should be used together other descriptors based on orbitals (such  $\Lambda$ )<sup>20</sup> or densities,<sup>22</sup> and the comparative analysis of all pieces of information will provide a deep understanding of the nature of the excited states and may be used as a reliable diagnostic.

## ■ ASSOCIATED CONTENT

### Supporting Information

Details on the TD-DFT excitations energies and corresponding diagnostic indexes, used for the statistics. This material is available free of charge via the Internet <http://pubs.acs.org>.

## ■ AUTHOR INFORMATION

### Corresponding Author

\*E-mail: [ciro.guido@ecp.fr](mailto:ciro.guido@ecp.fr) (C.A.G.); [carlo-adamo@chimie-paristech.fr](mailto:carlo-adamo@chimie-paristech.fr) (C.A.).

### Notes

The authors declare no competing financial interest.

## ■ ACKNOWLEDGMENTS

C.A.G. thanks Prof. David J. Tozer (Durham University) for the interesting discussion on the use of the  $\Lambda$ -index during the

IX Girona Seminar and Dr. Fabio Trani (EPFL) for stimulating discussions. The authors thank Prof. D. Jacquemin for providing the ground state structure of Triazene II. This work has been supported by the ANR agency under the Project DinFDFT (Project ANR 2010 BLANC n. 0425).

## ■ REFERENCES

- (1) (a) Laane, J. *Structure and Dynamics of Electronic Excited States*; Springer: Berlin, Germany, 1999; (b) Klessinger, M.; Michl, J. *Excited States and Photochemistry of Organic Molecules*; VCH: Weinheim, Germany, 1995.
- (2) O'Regan, B.; Grätzel, M. *Nature* **1991**, 353, 737–740.
- (3) Sandorfy, C. *Electronic Spectra and Quantum Chemistry*; Prentice-Hall: Englewood Cliffs, 1964.
- (4) Serrano-Andrés, L.; Merchán, M. *J. Mol. Struct.: THEOCHEM* **2005**, 729, 99–108.
- (5) Werner, H. J.; Schütz, M. *J. Chem. Phys.* **2011**, 135, 144116.
- (6) Runge, E.; Gross, E. K. U. *Phys. Rev. Lett.* **1984**, 52, 997–1000.
- (7) Jacquemin, D.; Perpète, E. A.; Ciofini, I.; Adamo, C. *Acc. Chem. Res.* **2009**, 42, 326–334.
- (8) Casida, M. E. Time-Dependent Density Functional Response Theory for Molecules. In *Recent advances in density functional methods*; Chong, D. P., Ed.; World Scientific: Singapore, 1995; Vol. 1, pp 155–193.
- (9) Cohen, A. J.; Mori-Sanchez, P.; Yang, W. T. *Science* **2008**, 321, 792.
- (10) Burke, K.; Werschnik, J.; Gross, E. K. U. *J. Chem. Phys.* **2005**, 123, 062206.
- (11) Dreuw, A.; Head-Gordon, M. *Chem. Rev.* **2005**, 105, 4009–4037.
- (12) Jacquemin, D.; Wathelet, V.; Perpète, E. A.; Adamo, C. *J. Chem. Theory. Comput.* **2009**, 5, 2420–2435.
- (13) Caricato, M.; Trucks, G. W.; Frisch, M. J.; Wiberg, K. B. *J. Chem. Theory. Comput.* **2010**, 6, 370–383.
- (14) Rohrdanz, M. A.; Herbert, J. M. *J. Chem. Phys.* **2008**, 129, 034107.
- (15) Goerigk, L.; Moellmann, J.; Grimme, S. *Phys. Chem. Chem. Phys.* **2009**, 11, 4611.
- (16) Goerigk, L.; Grimme, S. *J. Chem. Phys.* **2010**, 132, 184103.
- (17) Casida, M. E. *J. Mol. Struct.: THEOCHEM* **2009**, 914, 3–18.
- (18) Tozer, D. J.; Amos, R. D.; Handy, N. C.; Roos, B. J.; Serrano-Andrés, L. *Mol. Phys.* **1999**, 97, 859–868.
- (19) Adamo, C.; Barone, V. *Chem. Phys. Lett.* **1999**, 314, 152–157.
- (20) Peach, M. J. G.; Benfield, P.; Helgaker, T.; Tozer, D. J. *J. Chem. Phys.* **2008**, 128, 044118.
- (21) Ziegler, T.; Seth, M.; Krykunov, M.; Autschbach, J. *J. Chem. Phys.* **2008**, 129, 184114.
- (22) Le Bahers, T.; Adamo, C.; Ciofini, I. *J. Chem. Theory Comput.* **2011**, 7, 2498–2506.
- (23) Nitta, H.; Kawata, I. *Chem. Phys.* **2012**, 405, 93–99.
- (24) Bedard-Hearn, M. J.; Sterpone, F.; Rossky, P. J. *J. Phys. Chem. A* **2010**, 114, 7661–7670.



- (25) Plasser, F.; Lischka, H. *J. Chem. Theory Comput.* **2012**, *8*, 2777–2789.
- (26) Leang, S. S.; Zaharie, F.; Gordon, M. S. *J. Chem. Phys.* **2012**, *136*, 104101.
- (27) Kuhlman, T. S.; Mikkelsen, K. V.; Møller, K. B.; Sølling, T. I. *Chem. Phys. Lett.* **2009**, *478*, 127–131.
- (28) Peach, M. J. G.; Ruth Le Sueur, C.; Ruud, K.; Guillaume, M.; Tozer, D. J. *Phys. Chem. Chem. Phys.* **2009**, *11*, 4465–4470.
- (29) Perdew, J. P.; Schmidt, K. Jacob's ladder of density functional approximations for the exchange-correlation energy. In *Density Functional Theory And Its Application To Materials*; AIP Conference Proceedings; Antwerp, Belgium, June 8–10, 2000; AIP: 2001; Vol. 577, pp 1–20.
- (30) Kornobis, K.; Kumar, N.; Wong, B. M.; Lodowski, P.; Jaworska, M.; Andrzejewski, T.; Ruud, K.; Kozłowski, P. M. *J. Phys. Chem. A* **2011**, *115*, 1280–1292.
- (31) Dwyer, A. D.; Tozer, D. J. *Phys. Chem. Chem. Phys.* **2010**, *12*, 2816–2818.
- (32) Wiggins, P.; Williams, J. A. G.; Tozer, D. J. *J. Chem. Phys.* **2009**, *131*, 091101.
- (33) Peach, M. J.; Tozer, D. J. *J. Phys. Chem. A* **2012**, *116*, 9783–9789.
- (34) Peach, M. J.; Tozer, D. J. *J. Mol. Struct.: THEOCHEM* **2009**, *914*, 110–114.
- (35) Wong, B. M.; Hsieh, T. H. *J. Chem. Theory Comput.* **2010**, *6*, 3704–3712.
- (36) Richard, R. M.; Herbert, J. M. *J. Chem. Theory Comput.* **2011**, *7*, 1296–1306.
- (37) Kuritz, N.; Stein, T.; Baer, R.; Kronik, L. *J. Chem. Theory Comput.* **2011**, *7*, 2408–2415.
- (38) Foster, J. M.; Boys, S. F. *Rev. Mod. Phys.* **1960**, *32*, 300–302.
- (39) Boys, S. F. *Rev. Mod. Phys.* **1960**, *32*, 296–299.
- (40) Fang, H.; Bian, J.; Li, L.; Yang, W. *J. Chem. Phys.* **2004**, *120*, 9458–9466.
- (41) Smith, Q. A.; Ruedenberg, K.; Gordon, M. K.; Splipchenko, L. V. *J. Chem. Phys.* **2012**, *136*, 244107.
- (42) Frisch, M. J.; Trucks, G. W.; Schlegel, H. B.; Scuseria, G. E.; Robb, M. A.; Cheeseman, J. R.; Scalmani, G.; Barone, V.; Mennucci, B.; Petersson, G. A.; Nakatsuji, H.; Caricato, M.; Li, X.; Hratchian, H. P.; Izmaylov, A. F.; Bloino, J.; Zheng, G.; Sonnenberg, J. L.; Hada, M.; Ehara, M.; Toyota, K.; Fukuda, R.; Hasegawa, J.; Ishida, M.; Nakajima, T.; Honda, Y.; Kitao, O.; Nakai, H.; Vreven, T.; Montgomery, Jr., J. A.; Peralta, J. E.; Ogliaro, F.; Bearpark, M.; Heyd, J. J.; Brothers, E.; Kudin, K. N.; Staroverov, V. N.; Kobayashi, R.; Normand, J.; Raghavachari, K.; Rendell, A.; Burant, J. C.; Iyengar, S. S.; Tomasi, J.; Cossi, M.; Rega, N.; Millam, J. M.; Klene, M.; Knox, J. E.; Cross, J. B.; Bakken, V.; Adamo, C.; Jaramillo, J.; Gomperts, R.; Stratmann, R. E.; Yazyev, O.; Austin, A. J.; Cammi, R.; Pomelli, C.; Ochterski, J. W.; Martin, R. L.; Morokuma, K.; Zakrzewski, V. G.; Voth, G. A.; Salvador, P.; Dannenberg, J. J.; Dapprich, S.; Daniels, A. D.; Farkas, Ö.; Foresman, J. B.; Ortiz, J. V.; Cioslowski, J.; Fox, D. J. *Gaussian 09 Development Version*, Revision H.11; Gaussian, Inc.: Wallingford CT, 2009.
- (43) Guido, C. A.; Jacquemin, D.; Adamo, C.; Mennucci, B. *J. Phys. Chem. A* **2010**, *114*, 13402–13410.
- (44) Guido, C. A.; Knecht, S.; Kongsted, J.; Mennucci, B. *J. Chem. Theory Comput.* **2013**, *9*, 2209–2220.
- (45) Preat, J.; Michaux, C.; Lewalle, A.; Perpète, E. A.; Jacquemin, D. *Chem. Phys. Lett.* **2008**, *451*, 37–42.
- (46) Perdew, J. P.; Burke, K.; Ernzerhof, M. *Phys. Rev. Lett.* **1996**, *77*, 3865–3868.
- (47) Becke, A. D. *J. Chem. Phys.* **1993**, *98*, 1372–1377.
- (48) Lee, C. T.; Yang, W. T.; Parr, R. G. *Phys. Rev. B* **1988**, *37*, 785–789.
- (49) Tao, J.; Perdew, J. P.; Staroverov, V. N.; Scuseria, G. E. *Phys. Rev. Lett.* **2003**, *91*, 146401.
- (50) (a) Adamo, C.; Barone, V. *J. Chem. Phys.* **1999**, *110*, 6158–6170. (b) Ernzerhof, M.; Scuseria, G. E. *J. Chem. Phys.* **1999**, *110*, 5029–5036.
- (51) Stephens, P. J.; Devlin, F. J.; Chabalowski, C. F.; Frisch, M. J. *J. Phys. Chem.* **1994**, *98*, 11623–11627.
- (52) Becke, A. D. *J. Chem. Phys.* **1993**, *98*, 5648–5652.
- (53) Staroverov, V. N.; Scuseria, G. E.; Tao, J.; Perdew, J. P. *J. Chem. Phys.* **2003**, *119*, 12129–12137.
- (54) Cortona, P. *J. Chem. Phys.* **2012**, *136*, 086101. Guido, C. A.; Brémond, E.; Adamo, C.; Cortona, P. *J. Chem. Phys.* **2013**, *138*, 021104.
- (55) Vydrov, O. A.; Scuseria, G. E. *J. Chem. Phys.* **2006**, *125*, 234109.
- (56) Krukau, A. V.; Scuseria, G. E.; Perdew, J. P.; Savin, A. *J. Chem. Phys.* **2008**, *129*, 124103.
- (57) Yanai, T.; Tew, D. P.; Handy, N. C. *Chem. Phys. Lett.* **2004**, *393*, 51–57.
- (58) Rohrdanz, M. A.; Martins, K. M.; Herbert, J. M. *J. Chem. Phys.* **2009**, *130*, 054112.
- (59) Benchmark Assessment Repository. <http://www.dur.ac.uk/d.j.tozer/excite3.html> (accessed January 10, 2013).
- (60) Stein, T.; Kronik, L.; Baer, R. *J. Am. Chem. Soc.* **2009**, *131*, 2818–2820.
- (61) Tawada, Y.; Tsuneda, T.; Yanagisawa, S.; Yanai, T.; Hirao, H. *J. Chem. Phys.* **2004**, *120*, 8425–8433.
- (62) Jacquemin, D.; Ciofini, I.; Perpète, E. A.; Adamo, C. *Theor. Chem. Acc.* **2011**, *128*, 127–136.
- (63) Ciofini, I.; Adamo, C. *J. Phys. Chem. A* **2007**, *111*, 5549–5556.